Journal of Colloid and Interface Science 581 (2021) 533–544

Contents lists available at ScienceDirect

Journal of Colloid and Interface Science

journal homepage: www.elsevier.com/locate/jcis

Bioflocculants from wastewater: Insights into adsorption affinity, flocculation mechanisms and mixed particle flocculation based on biopolymer size-fractionation

Victor Ajao [a,b,*], Remco Fokkink [c], Frans Leermakers [c], Harry Bruning [b], Huub Rijnaarts [b], Hardy Temmink [a,b]

[a] Wetsus – European Centre of Excellence for Sustainable Water Technology, P.O. Box 1113, 8911 CC Leeuwarden, Netherlands
[b] Department of Environmental Technology, Wageningen University and Research, P.O. Box 8129, 6700 EV Wageningen, Netherlands
[c] Physical Chemistry and Soft Matter, Wageningen University and Research, P.O. Box 8038, 6700 Wageningen, Netherlands

HIGHLIGHTS

- Size-based characterisation helped to understand how EPS flocculate particles.
- Different EPS fractions showed different adsorption kinetics and binding affinities.
- Optical reflectometry revealed site-blocking effect in mixed EPS.
- Mixed EPS flocculated particle mixtures better than the high-MW EPS fraction.

GRAPHICAL ABSTRACT

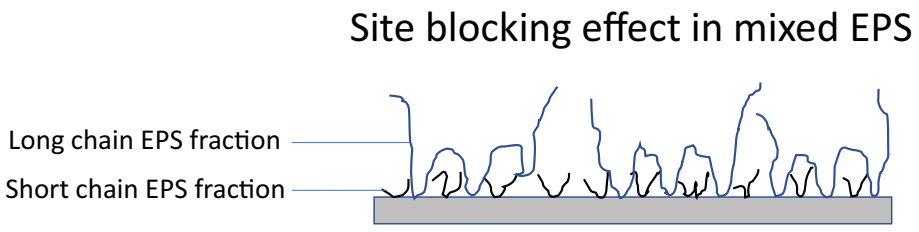

ARTICLE INFO

Article history:
Received 10 April 2020
Revised 29 July 2020
Accepted 30 July 2020
Available online 2 August 2020

Keywords:
Co-adsorption
Dual clay system
Extracellular polymeric substances
Kaolinite
Montmorillonite
Natural flocculants
Polymer adsorption
Polymer mixture
Optical reflectometry
Site blocking

ABSTRACT

Hypothesis: Microbial extracellular polymeric substances (EPS) produced from wastewater are generally heterodispersed, which is expected to influence their flocculation performances and mechanism, particularly in mixed particle systems. The different molecular weight (MW) fractions should contribute to the overall adsorption affinity and flocculation mechanism of EPS in single and dual clay systems.
Experiments: EPS harvested from bioreactors were size-fractionated into high, medium and low MW fractions (HMW, MMW, LMW, respectively). The harvested mixed EPS and its fractions were characterised by diverse analytical techniques coupled with optical reflectometry to investigate the role of each EPS fraction in the overall flocculation mechanism of EPS in kaolinite and montmorillonite clay systems.
Findings: In single clay systems, both the harvested mixed EPS and the HMW-EPS fraction showed comparable flocculation performances. However, mixed EPS proved to be more efficient than the HMW-EPS fraction for dual clay flocculation. Site blocking effects were observed in mixed EPS: the LMW and MMW EPS first adsorbed to the surface due to higher diffusivities and faster mass transfer to the interface, while the HMW-EPS were slowly transported but were attached to the surface irreversibly and stronger than the LMW/MMW-EPS. We propose from this, a mixed EPS adsorption mechanism: extended anionic polymer tails in solution, thereby enhancing particle flocculation.

Abbreviations: BET, Brunauer-Emmett-Teller; BSA, Bovine Serum Albumin; CD, Charge density; COD, Chemical oxygen demand; EPS, Extracellular polymeric substances; FE, Flocculation efficiency; FTIR, Fourier transform infrared; LC-OCD, Liquid chromatography-organic carbon detection; LMW, Low molecular weight; MBR, Membrane bioreactor; MW, Molecular weight; MWCO, Molecular weight cut-off; NLDFT, Non-Local Density Functional Theory; NTU, Nephelometric turbidity unit; pDADMAC, polydiallyldimethylammonium chloride; S-EPS, Soluble extracellular polymeric substance.

* Corresponding author at: Wetsus – European Centre of Excellence for Sustainable Water Technology, P.O. Box 1113, 8911 CC Leeuwarden, Netherlands.
E-mail addresses: Victor.ajao@wetsus.nl (V. Ajao), remco.fokkink@wur.nl (R. Fokkink), frans.leermakers@wur.nl (F. Leermakers), harry.bruninig@wur.nl (H. Bruning), huub.rijnaarts@wur.nl (H. Rijnaarts), hardy.temmink@wur.nl (H. Temmink).

https://doi.org/10.1016/j.jcis.2020.07.146
0021-9797/

1. Introduction

The coagulation/flocculation process has been employed for centuries as a simple and effective way to destabilise, agglomerate and remove particles from water and wastewater. Currently, this process is widely achieved with the use of inorganic coagulants and fossil-based organic flocculants. Flocculants are particularly important because they are efficient at low dosages and able to form strong flocs [1]. However, most synthetic flocculants biodegrade poorly and some of the degradation products/monomer residues are toxic, with acrylamide from polyacrylamide as a well-known example [1]. Hence, their application in open systems such as dredging and tunnelling pose a risk on humans, aquatic animals and the environment [2].

As an alternative, bioflocculants have gained increasing attention for water treatment due to their biodegradability, non-toxic property, and effective flocculation performances sometimes comparable with synthetic flocculants [3–7]. Quite recently, microbial extracellular polymeric substances (EPS) are being explored as promising bioflocculants due to their relatively high molecular weight [7–9]. EPS are products of microbial biochemical secretions and may either be produced by pure or mixed cultures. The usual approach is the enrichment of pure cultures with single organic substrates (such as glucose) to obtain a single type of EPS, usually polysaccharides [8,10–12]. Although this strategy produces biodegradable EPS, the disadvantage is that it necessitates sterile conditions and expensive carbon sources. On the contrary, a mixed-culture approach requires no sterility and can be fed with low-cost feedstocks such as organic wastewater. One outcome of the mixed-culture approach is the production of a heterogeneous and heterodispersed EPS matrix, comprising different compounds with different molecular weights (MWs) and charge densities (CDs) [7,13]. These two characteristics (MW and CD), especially the former, govern the flocculation process and performance of anionic flocculants such as EPS [14]. Previous studies reported wastewater-produced EPS to comprise a mixture of varying MWs [7,13,15,16], which according to Bolto and Gregory [17], can be generally classified as high (>1000 kDa), medium (1000–100 kDa) and low (<100 kDa) MW fractions.

MW polymers have been reported to favour polymer bridging between particles since such molecules expand further in suspension ($\gg$50 nm [18]), escape the electrostatic field of the attached particle (generally < 50 nm at ionic strengths in wastewater [18]), adsorb on other particles and result in big and fast-settling flocs [14]. However, very high MW (typically > 15 MDa) can have an adverse effect on adsorption and flocculation. Such polymers tend to have fewer chains per gram (specifically for linear polymers), a higher chain entanglement and result in a highly viscous polymer solution that is poorly distributed in suspension [19]. In the last few decades, the use of polymer mixtures, especially dual-polymer systems (low and high MW or medium and high MW polymers) has gained considerable interest due to some significant advantages over the use of single-type polymers [14]. The studied dual-polymer systems typically involved a cationic low MW polymer and a subsequent anionic high MW polymer [14,20–22]. The advantage of this approach is the synergistic effect of two flocculation mechanisms – charge neutralisation by the cationic polymer and bridge formation by the anionic polymer [14,20]. While the polycation adsorbs to the particles via electrostatic interaction, it also provides adsorption sites for the polyanion to form bridges with itself and other particles [14]. For instance, Yu and Somasundaran [20] showed that by pre-adsorbing polydiallyldimethylammonium chloride (pDADMAC, 240 kDa) on alumina particles, the subsequent adsorption of polyacrylic acid (PAA, 100 kDa) was enhanced and the settling rate tripled compared to the addition of pDADMAC alone. In the same vein, Fan et al. [23] reported that the use of a dual polymer system (cationic Percol, 1.8 MDa and anionic PAA, 10 kDa) increased the turbidity removal efficiency of alumina particles by 11–15 % compared to the sole use of PAA, and by 30–33 % compared to the use of Percol.

Wastewater-produced EPS comprise a mixture of different MW fractions (mixed EPS consisting of high, medium and low MW fractions) and have also been reported to show excellent flocculation of particles with performances comparable to some synthetic flocculants such as anionic polyacrylamide [7]. Due to the net negative charge of EPS [7], polymer bridging (particularly divalent cationic bridging) has been proposed and reported as the flocculation mechanism – a phenomenon also found in synthetic anionic flocculants [17,24]. However, there has been no report on the role of each MW fraction on the overall flocculation mechanism. More so, the use of (synthetic) polymer mixtures composed of anionic polymers is yet to be studied. The advantage of such mixtures (and in this case, mixed EPS) may be the synergistic effect of these MW fractions on single or mixed suspensions or the ability of different fractions to selectively adsorb to different particles in a mixture. We conjectured that in the presence of di/multi-valent cations, the low MW (LMW) EPS fraction would (preferentially) adsorb to the smaller particles in a mixture while the high MW fractions will bridge to the tails of the adsorbed LMW EPS and adsorb to the bigger particles.

To study polymer adsorption in a controlled system, optical reflectometry has been reported as an effective technique [25–27]. With this technique, we can monitor the *in situ* adsorption of polymers on a flat reflective surface in a stagnation point flow cell. Due to its high sensitivity and controlled hydrodynamic condition, it is possible to determine (low) amounts of adsorbed polymers and to characterise the kinetics of adsorption. As reported by Wågberg and Nygren [27], the combination of optical reflectometry with flocculation measurements can be very powerful in gaining insights into the working mechanism of flocculants.

This study, for the first time, investigates the effect of the different MW fractions of EPS on single and dual clay (kaolinite and montmorillonite as models) particle flocculation and mechanism of flocculation. We imagined that mixed EPS would better flocculate a mixture of particles than a single MW EPS. Optical reflectometry was used to observe the *in situ* adsorption of the different MW fractions on a flat silica surface, from which we could determine the adsorption affinity and kinetics of each fraction and mixtures of fractions. From these experiments, we elucidated the mechanism on how the various MW fractions of EPS adsorb to single and dual clay mixtures.

2. Materials and methods

2.1. Production, harvesting and fractionation of EPS

A submerged membrane bioreactor (MBR) with a working volume of 3.3 L was operated to produce EPS. The MBR operation, wastewater composition (fresh wastewater consisting of glycerol and ethanol at a COD/N ratio of 100) and EPS yield have been thoroughly described elsewhere [28]. During the steady-state reactor operation, soluble (S)-EPS were harvested from the reactor content, having been reported to be the major EPS fraction (62–77 wt%) when operating a reactor under nitrogen-limited conditions [28]. S-EPS were harvested via centrifugation: 1000 mL sludge was centrifuged at 17,000 g and 4 °C for 1 h, after which the supernatant containing the S-EPS (henceforth called 'mixed EPS') was dialysed (tubular dialysis membrane, 12–14 kDa molecular weight cut-off,

MWCO – Spectra/Por 2) against demineralised water to remove salts and ultra-low MW compounds.

Dialysed mixed EPS were size-fractionated into three MW fractions (Fig. 1) using membrane filters (with different MWCO) fitted in Amicon® dead-end filtration cells operated at 2.5 bars. The first filtration was performed using a 0.1 μm hydrophilic polyethersulfone membrane disc (Pall Corporation, Supor®). The retentate was collected by carefully scraping and washing (with demineralised water) the biopolymer film on the membrane. The permeate was further filtered using a 100 kDa polysulfone membrane (Microdyn Nadir PM US100) and the retentate and permeate were collected separately. The 0.1 μm membrane retentate, 100 kDa membrane retentate and 100 kDa membrane filtrate were classified as high, medium and low MW (HMW, MMW and LMW) EPS fractions, respectively. Each fraction and the mixed EPS were frozen at −80 °C and freeze-dried.

2.2. EPS characterisation

2.2.1. Molecular weight and charge density measurement

The mixed EPS and its fractions were further analysed for MW using liquid chromatography-organic carbon detection (LC-OCD – model 8, DOC-LABOR, Germany). The detailed method has been described by Ajao *et al.* [28]. Prior to the analysis, each sample was dissolved in Milli-Q water and passed through a 0.45 μm hydrophilic polytetrafluoroethylene filter.

The CDs were determined by colloid titration using a Mütek Particle Charge Detector (PCD03, Germany) described by Tan *et al.* [29] and a titration procedure explained by Ajao *et al.* [7]. The CDs were determined at a sample solution pH of 7.0 ± 0.1 (because the clay suspensions were prepared at this pH) and calculated from the titrant (pDADMAC) consumption according to the equation:

$$q = \frac{c * V}{m} \quad (1)$$

where q is the specific charge quantity (eq/g), c is the titrant concentration (eq/L), V is the consumed titrant volume (L), and m is the mass of the sample (g).

2.2.2. Functional group determination

Fourier transform infrared spectroscopy (FTIR) was carried out on the freeze-dried EPS samples using an IRTracer-100 spectrometer (Shimadzu, Japan) with a scanning range of 4000–450 cm^{-1} for 40 scans at a spectral resolution of 4 cm^{-1}.

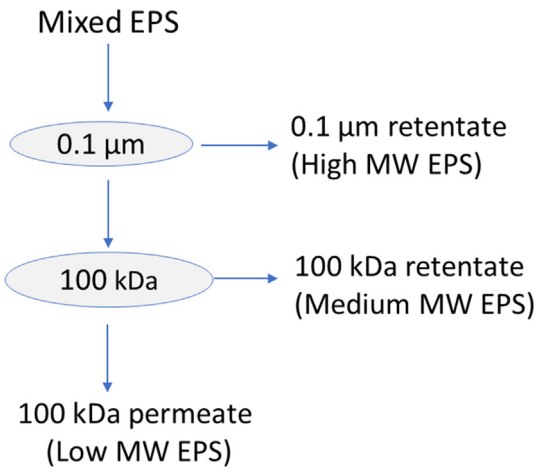

Fig. 1. Mixed EPS fractionation into the three molecular weight fractions – high, medium and low molecular weight fractions.

2.2.3. Total protein and polysaccharide quantification

Previous studies under the same conditions reported polysaccharides and proteins as the main components of (soluble) EPS [28,30]. Hence, each component was measured colorimetrically to determine the total protein and polysaccharide content.

The total protein content of the dried EPS samples was determined using a bicinchoninic acid (BCA) assay kit (Thermo Scientific, USA). The assay was performed in a microplate, where 25 μL of EPS solution (dissolved in a phosphate buffer saline, pH 7.4 [28]) or bovine serum albumin, BSA (used as a standard protein) was mixed with 200 μL of BCA working reagent and incubated at 37 °C for 30 min. Afterward, the absorbance was measured at 570 nm using a spectrophotometer (Victor3 1420 Multilabel Counter, Perkin Elmer, USA).

Total polysaccharides were quantified using the phenol–sulphuric acid method described by Dubois et al. [31], using glucose (purchased from Sigma Aldrich, Netherlands) as the standard sugar. Absorbance was measured at 490 nm in the spectrophotometer mentioned above.

2.3. Clay characteristics and flocculation tests

Flocculation tests were carried out in a jar test flocculation unit, as described by Ajao et al. [8]. Naturally occurring kaolinite (purchased from Sigma Aldrich, Netherlands) and montmorillonite (purchased from VWR, Netherlands) were used as model particles. These clay particles were selected due to their different characteristics (Table 1), to mimic mixed particles in natural environments. Although kaolinite is the most common clay in many dredging, mining and oil sand operations, other clay types such as montmorillonite are also major components [32]. Montmorillonite behaves differently from kaolinite because of its swelling character, which is attributed to the Na^+ and Ca^{2+} exchange on the clay surface. The swollen clay retains much water and contributes to the poor dewaterability of tailings ponds [32]. For this reason, montmorillonite suspensions are also important model systems to investigate.

We investigated the potential of the harvested mixed EPS, its fractions and the combination of fractions to flocculate single and dual clay mixtures. For this purpose, three clay suspensions (a working volume of 100 mL) were prepared: (i) 5 g/L kaolinite suspension, as extensively used in several studies to determine the flocculation performance of EPS [9] (ii) 1.5 g/L montmorillonite suspension [33] – a lower montmorillonite concentration was used due to its swelling property, and (iii) a mixture of kaolinite and montmorillonite (1.5 g/L each). Each suspension was prepared in Milli-Q water, stirred overnight and neutralised to pH 7 by adding a few drops of NaOH. EPS samples were also dissolved in Milli-Q water at a concentration of 0.1 g/L.

First, we determined for each EPS fraction and the mixed EPS the optimum concentration required to best flocculate each clay. (As shown later in Section 3.5.1, the flocculation tests were carried out in a 'starved' polymer regime, i.e., an excess particle surface area compared to the polymer dosage.) From this result, the best performing EPS fractions, different combinations of fractions and the mixed EPS were investigated for mixed particle flocculation. In all the tests, 100 mg/L Ca^{2+} (from $CaCl_2{\cdot}2H_2O$) was added as a coagulant to reduce the electrostatic repulsion between the negatively charged clay particles and to facilitate bridging between the anionic particles and EPS [7,28]. (About this Ca^{2+} concentration is frequently observed in natural waters.) After 5 mins of settling, the supernatant turbidity after flocculation was measured with a turbidimeter (2100 N IS, Hach) in Nephelometric Turbidity Units (NTU). Flocculation efficiency (*FE*) was calculated as follows:

Table 1
Clay characteristics.

Kaolinite	Montmorillonite
($Al_2O_3{\cdot}2SiO_2{\cdot}2H_2O$)	$(Na,Ca)_{0.33}(Al,Mg)_2(Si_4O_{10})(OH)_2{\cdot}nH_2O$
1:1 clay: 1 silica tetrahedral sheet and 1 alumina octahedral sheet	2:1 clay: 2 silica tetrahedral sheets and 1 alumina octahedral sheet
Layers held by hydrogen bond – restricts expansion	Layers held by van der Waals bond
Low swelling capacity	High swelling capacity
Low cation exchange capacity, (~0.09 meq/g)	High cation exchange capacity (~1 meq/g) [34]
Volume-based particle size: 2.93 ± 1.51 μm [a]	Particle size (after swelling): 5.97 ± 2.51 μm [a]
Surface area (BET): 7.52 m^2/g [b]	Surface area (BET): 25.68 m^2/g [b]
Total pore area (NLDFT): 5.75 m^2/g [b]	Total pore area (NLDFT): 19.10 m^2/g [b]

[a] Particle size was measured using a DIPA 2000 (Doner Technologies, Israel) in triplicates.
[b] Surface area and porosity were determined using a Micromeritics Tristar 3000 (USA) in triplicates. The detailed method has been described by Suresh Kumar *et al.* [35]. BET: Brunauer-Emmett-Teller; NLDFT: Non-Local Density Functional Theory.

$$FE(\%) = \frac{NTU_{control} - NTU_{test}}{NTU_{control}} * 100 \quad (2)$$

where $NTU_{control}$ is the turbidity value of the control experiment (without EPS addition but with Ca^{2+} addition; supernatant turbidity = 210 ± 10 NTU for kaolinite and 100 ± 10 NTU for montmorillonite), and NTU_{test} is the turbidity value of test experiment (with Ca^{2+} and EPS added). The supernatant was also analysed with LC-OCD to measure the biopolymer organic carbon [7] that was not adsorbed in the flocs (supernatant-phase EPS concentration or non-adsorbed EPS concentration), and by subtracting this from the total dosed EPS concentration, we obtained the fraction of EPS adsorbed (adsorbed EPS). Additionally, the zeta (ζ) potential of the supernatants, clay suspensions and EPS were calculated from electrophoretic measurements (Malvern Mastersizer 2000, UK) using the Smoluchowski equation [36]. It is important to note that the ζ potential is not affected by the clay concentration [36]. All experiments and analyses were done in at least duplicates.

2.4. Optical reflectometry test

A stagnation point optical reflectometer (manufactured by the Laboratory of Physical Chemistry and Soft Matter of Wageningen University, Netherlands) was used to determine the adsorbed amount and build-up behaviour of the EPS fractions. A full description of the device and its underlying theory have been thoroughly described elsewhere [25,37], but in the supplementary material, there is a detailed description of the stagnation point region. Reflectometry is an optical technique used to observe the in situ adsorption of molecules on an optically flat surface, such as a silicon wafer. The changes in signal measured upon adsorption on the surface (ΔS) is directly proportional to the adsorbed amount, Γ (mg/m^2) according to the equation:

$$\Gamma = Q_f \frac{\Delta S}{S_0} \quad (3)$$

where *S*0 is the starting output signal of the bare silicon wafer, $\Delta S = S - S0$ is a change in the signal upon adsorption on the surface, and Q_f (mg/m^2) is the sensitivity factor, calculated with the *Prof. Huygens* v1.3 program (Dullware software) using the refractive index increments (dn/dc) of the adsorbate (in this case, EPS). To determine the d*n*/d*c*, the refractive indexes (*n*) of mixed EPS at different concentrations (*c* = 0.5, 1.0, 2.5, 5, 10, 15, 20 g/L; dissolved in Milli-Q water) were measured at room temperature (21 ± 1 °C) using a J47 refractometer (Rudolph, USA). The d*n*/d*c*, which is the slope of *n versus c* was obtained as 0.135 mL/g (see Supplementary material, Fig. S1), a value close to that of poly(ethylene oxide), the most studied polymer in optical reflectometry ($dn/dc_{poly(ethylene\ oxide)}$ = 0.134 mL/g).

Since both kaolinite and montmorillonite clays (and most clay particles) are silica-based, the reflectometry tests were performed on a silica surface, which is largely representative of most clay types. Silicon wafers (obtained from Wafernet, USA) were heated at 1000 °C for 1 h to form an oxide layer of silica. The oxidised wafers with a silica layer thickness of 70 ± 10 nm (measured by ellipsometry) were cut into strips of approximately 1 × 4 cm^2, immersed in a freshly prepared piranha solution (1 part of 30% H_2O_2 and 3 parts of 95% H_2SO_4) for 20 min and rinsed in Milli-Q water.

Each adsorption measurement typically involved a wafer being placed in the reflectometer cell, rinsed with a solvent (5 mM Ca^{2+}, except stated otherwise) to establish the baseline signal (*S0*), followed by the introduction of an EPS sample solution and its adsorption was monitored, in most cases, until a plateau was reached. In some cases, this was followed by rinsing with the same solvent until a new plateau was reached, and in other cases, another EPS sample solution was directly introduced. All reported values were calculated based on the amounts that remained adsorbed on the surface after rinsing with the solvent (referred to as the irreversible adsorbed amounts) unless mentioned otherwise. All EPS samples were tested at pH 7.

3. Results

3.1. EPS characteristics

3.1.1. Composition and functional groups

FTIR analysis was carried out to compare the chemical composition of the mixed EPS (the harvested soluble-EPS) and its fractions (Fig. 2). The mixed EPS, HMW EPS and MMW EPS showed similar absorption bands (interpreted in Table 2), revealing the presence of polysaccharides and proteins as the main components. Although this FTIR analysis mainly gives qualitative information, a clear difference is observed between the LMW EPS spectrum and the other spectra. The typically broad and sharp O—H stretching vibrations at around 3282 cm^{-1} was rather obscure for the LMW EPS. Similarly, the band at 1018 cm^{-1} (C—O—C asymmetric stretching) was noticeably smaller in the LMW EPS spectrum compared to the other spectra that have sharp and distinct peaks. These two groups are associated with carbohydrates, suggesting that the LMW EPS have a much lower polysaccharide content than the MMW and HMW fractions (confirmed later by other characterisation techniques). On the other hand, the amide III band at 1396 cm^{-1} was more conspicuous in the LMW EPS spectrum than the other spectra, signifying a higher protein content in the LMW EPS than the other EPS fractions. The fingerprint region between 866 and 650 cm^{-1} (found only in the LMW EPS spectrum) is associated with the ring vibrations from aromatic amino acids and nucleotides [38].

Further quantification of the total polysaccharide and protein content is given in Table 3. The mixed EPS were composed of about 76 wt% biopolymers and the remaining 24 wt% accounts for non-biopolymeric components such as building blocks, low molecular weight acids and neutrals [7]. Out of the 76% biopolymers, 65 ± 3 wt% were polysaccharides and the remaining 11 ± 2 wt% were composed of proteins. The polysaccharides could be further fractionated into approximately 36 wt% HMW, 28 wt% MMW, and 3 wt% LMW fractions (MW characterisation on Table 3). The reverse trend was observed for the protein fractionation, which is

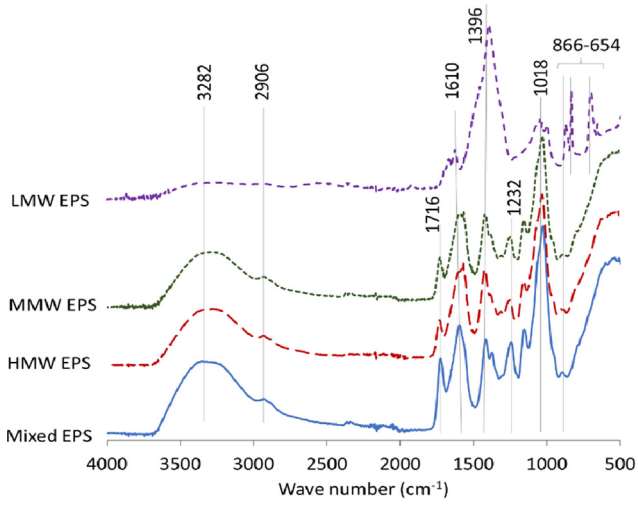

Fig. 2. FTIR spectra of mixed EPS and its fractions – HMW (high molecular weight), MMW (medium molecular weight) and LMW (low molecular weight).

Table 2
Band assignment for the FTIR spectral features of mixed EPS and its fractions [38–40].

Wavenumber (cm^{-1})	Functional group assignment
3282	O—H stretching vibrations
2906	C—H stretching vibration
1716	C=O stretching vibration of protein amide I band
1610	Out-of-phase N—H bending and C—N stretching vibrations of protein amide II band
1396	In-phase N—H bending of protein amide III band
1365	C=O symmetric stretching of $-COO^-$ groups
1232	C—O stretching of alcohol
1018	C—O—C asymmetric stretching of ester linkage of polysaccharides
866–654	Ring vibrations from aromatic amino acids and nucleotides

consistent with the FTIR result in Fig. 2: out of the 11 wt% EPS proteins, the fractions comprised 3 wt% HMW, 4 wt% MMW and 5 wt% LMW proteins. Hence, the order of the polysaccharide/protein ratio was HMW > MMW > LMW (Table 3). Apparently, polysaccharides were the main constituents in the high and medium MW EPS fractions while the LMW EPS fraction contained more proteins than polysaccharides.

3.1.2. Molecular weight and charge density

The average MW of the mixed EPS and its fractions are also presented in Table 3. The high MW of the mixed EPS (1.68 MDa) is similar to that previously reported [28], showing the possibility to obtain consistent EPS MW under similar operational conditions. A further size-fractionation of the mixed EPS reveals that the high, medium and low MW fractions have average MW values of 1.99, 0.78 and 0.13 MDa, respectively. The obtained MW value for the smallest EPS fraction (0.13 MDa) was however higher than the membrane's MWCO (0.1 MDa), indicating that some pores were larger than the manufacturer's reported average MWCO.

Each MW fraction possesses functional groups (particularly carboxyl and amine groups from polysaccharides and proteins) that are responsible for their charge. The charge density (CD) values in Table 3 are directly proportional to the polysaccharide/protein ratios: the HMW EPS with the highest ratio (12) have the highest CD value (6.46 meq/g). Likewise, the LMW EPS have the lowest CD value (1.30 meq/g). These findings imply that the EPS polysaccharides (with functional groups OH and $—COO^-$) gave a higher contribution to the anionic CD than the proteins (with functional groups NH_2 and $—COO^-$), which is consistent with other studies [28,41].

3.2. Flocculation in single clay systems

Flocculation tests were performed on kaolinite and montmorillonite suspensions separately, with the addition of 100 mg/L Ca^{2+} as a coagulant. A preliminary test without Ca^{2+} addition showed no flocculating effect and even led to negative flocculation efficiency values. The flocculation efficiencies of mixed EPS and its fractions toward these clay particles, in the presence of Ca^{2+}, are given in Fig. 3A and B. Clearly, the sole use of the LMW EPS showed poor flocculation of both kaolinite and montmorillonite particles. Above 0.5 mg LMW EPS/g kaolinite (1.0–20.0 mg/g kaolinite – results not shown), negative flocculation efficiencies were even obtained. At the optimum dosage of 0.2 mg/g kaolinite and 1.0 mg/g montmorillonite, the maximum flocculation efficiencies with LMW EPS were only 12% and 19%, respectively. In contrast, the MMW, HMW and mixed EPS exhibited good flocculation of kaolinite particles with average efficiencies of 87.4, 93.9, and 92.9% respectively, each at an (estimated) optimum dosage of 0.1 mg/g kaolinite (supernatant turbidity: 14 ± 3 NTU). This dosage is similar to the optimum dosage reported for some anionic polyacrylamide [7,42] and a bioflocculant produced by *Bacillus agaradhaerens* C9 [12], but much lower than values reported from some other studies (Sam et al. [43] – 400 mg EPS/g kaolin, Cosa et al. [44] – 50 mg/g kaolin, Li et al. [45] – 10 mg/g kaolin, who all used bioflocculants from isolated bacterial strains).

Above the optimum dosage, flocculation performances decreased, likely caused by the restabilisation of clay particles. Although the HMW EPS showed the highest efficiency with kaolinite (93.9%), the performance of mixed EPS was not significantly lower (92.9%).

With montmorillonite, higher flocculation efficiencies were obtained compared to kaolinite. The highest average performances of the MMW, HMW, and mixed EPS were 98.3, 98.9, and 97.7%, respectively, at a dosage of 0.5 mg/g montmorillonite (supernatant turbidity: 1.7 ± 0.5 NTU). Above this dosage, up to 2.5 mg/g, the flocculation efficiencies remained relatively constant for each EPS type. Thus, in contrast to kaolinite, the restabilisation effect was not observed with montmorillonite at higher dosages.

Table 3
Properties of mixed EPS and its fractions – HMW (high molecular weight), MMW (medium molecular weight) and LMW (low molecular weight). Values of polysaccharides and proteins are mean ± standard deviations of triplicate assays. Values of MW and CD are mean ± standard deviations of duplicate measurements.

Parameter	Mixed EPS	HMW EPS	MMW EPS	LMW EPS
Polysaccharide content [a] (g/g EPS)	0.65 ± 0.03	0.36 ± 0.04	0.28 ± 0.03	0.03 ± 0.00
Protein content [b] (g/g EPS)	0.11 ± 0.02	0.03 ± 0.01	0.04 ± 0.01	0.05 ± 0.01
Polysaccharide/protein ratio	6	12	7	0.6
Average molecular weight (MDa)	1.68 ± 0.15	1.99 ± 0.05	0.78 ± 0.03	0.13 ± 0.01
Charge density at pH 7 (meq/g)	5.10 ± 0.15	6.46 ± 0.12	5.12 ± 0.12	1.30 ± 0.11

[a] Based on glucose equivalent units.
[b] Based on BSA equivalent units.

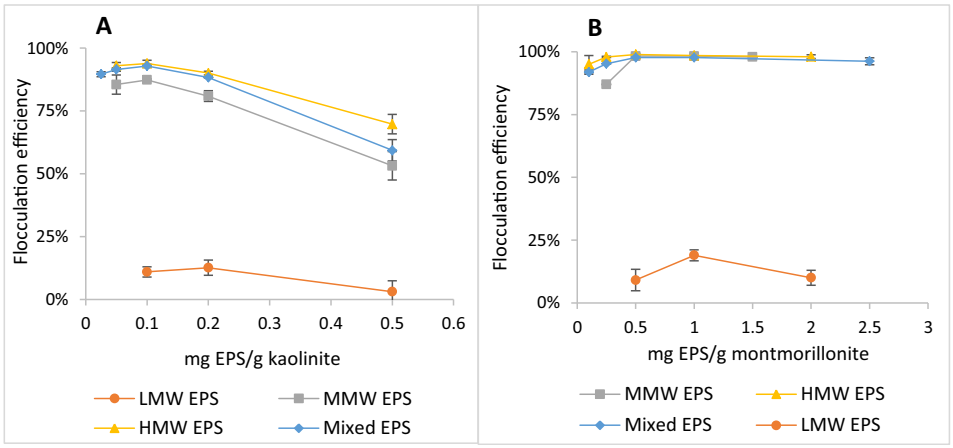

Fig. 3. Flocculation performances of mixed EPS and its fractions (with 100 mg/L Ca^{2+}) on kaolinite (A) and montmorillonite (B) clays. Tests were performed in duplicates.

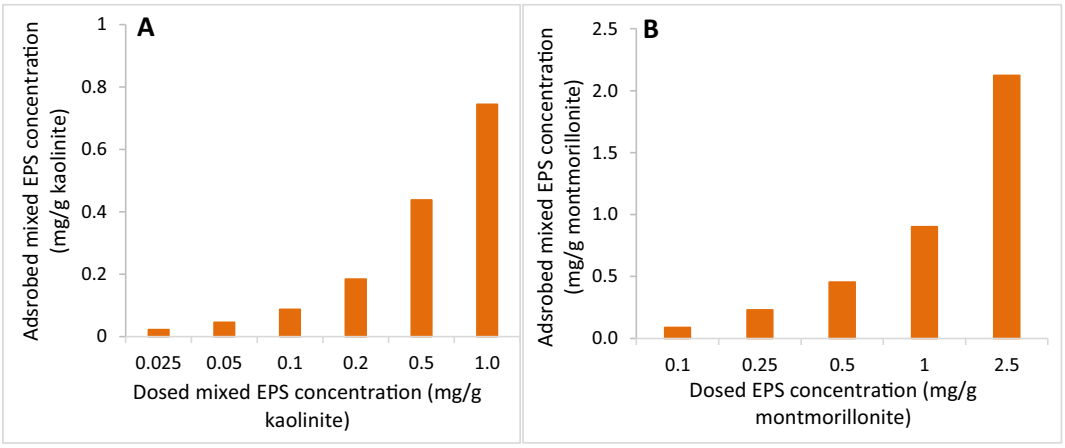

Fig. 4. The dosed mixed EPS concentration compared to the adsorbed mixed EPS concentration. (A) Kaolinite flocculation, (B) Montmorillonite flocculation.

The relationship between the dosed and adsorbed mixed EPS concentrations are presented in Fig. 4. At EPS dosages above 0.5 mg/g clay, an increasing surface saturation starts to become apparent since the amount adsorbed becomes significantly smaller than the amount dosed. The adsorbed EPS concentrations required to achieve the best flocculation performance were 0.09 mg/g kaolinite and 0.46 mg/g montmorillonite. These two values are close to the dosed mixed EPS concentrations of 0.1 mg/g kaolinite and 0.5 mg/g montmorillonite, respectively, demonstrating that, at the optimum dosages, 90% of the dosed mixed EPS was adsorbed on the kaolinite flocs and 92% was adsorbed on the montmorillonite flocs. These adsorbed concentrations (0.09 mg/g kaolinite and 0.46 mg/g) correspond to surface coverage areas of 0.012 mg/m^2 kaolinite and 0.018 mg/m^2 montmorillonite (using the BET values on Table 1). The higher coverage area for montmorillonite may have contributed to the higher flocculation performance compared to kaolinite flocculation performance.

3.3. Dual clay flocculation

The optimum flocculation dosages of each EPS fraction on kaolinite and montmorillonite were used to flocculate a 1:1 mixture of both clays (1.5 g/L each). Additionally, flocculation tests were carried out to determine the optimum concentrations for the mixed particles. The results are presented in the Supplementary material – Table S1. The main findings, illustrated in Fig. 5, show the effect of different EPS mixtures on mixed particle flocculation. With the HMW EPS (0.5 mg/g), a flocculation efficiency of 95.7% was achieved. At an equal dosage of the LMW and HMW EPS fractions (0.5 mg/g each), the efficiency was 96.2%. At equal concentrations (0.25 mg/g each) of the MMW and HMW EPS, the flocculation performance was 98%, and with the harvested mixed EPS, the efficiency was 98.7% at a dosage of 0.25 mg/g (supernatant

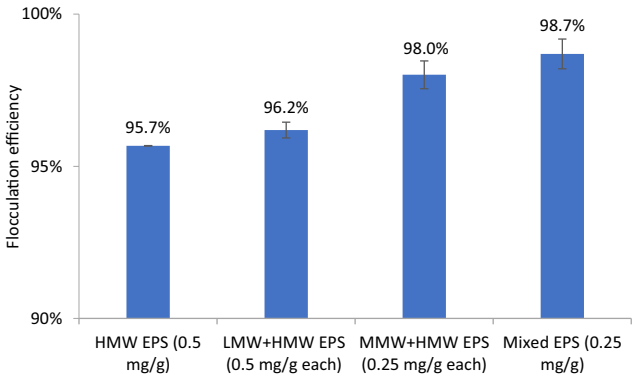

Fig. 5. Flocculation performance of mixed EPS and its fractions (with 100 mg/L Ca^{2+}) on a 1:1 mixture of kaolinite and montmorillonite clays at the optimal EPS concentrations. Tests were performed in duplicates.

turbidity: 2.3 ± 0.3 NTU). These results show that, with a mixture of MW fractions, the flocculation of mixed clay particles could be increased compared to using a single MW fraction (HMW EPS). Furthermore, the lower dosage required by the mixed EPS compared to the single MW fraction and the dual EPS mixtures is beneficial from a practical point of view.

3.4. EPS adsorption on a silica surface

While the jar tests of the clay particles provide useful information on the flocculation performances of the EPS (fractions), other important parameters such as the adsorption kinetics and the understanding of how each EPS fraction contributes to particle adsorption cannot be obtained by jar tests, hence optical reflectometry was employed (described in Sections 1 and 2.4).

3.4.1. Effect of calcium concentration

Since both the silica surface and EPS (fractions) were negatively charged, the addition of cations, especially divalent cations, was needed to reduce the electrostatic repulsion. Hence, the adsorption tests were carried out for all the EPS samples dissolved in a $CaCl_2 \cdot 2H_2O$ solution.

First, we established the optimum Ca^{2+} concentration needed for maximum irreversible adsorption (undesorbed EPS after rinsing the silica surface with the solvent) of EPS on the silica surface. Fig. 6 shows the adsorbed amount of mixed EPS at different Ca^{2+} concentrations – 100, 200, and 400 mg/L Ca^{2+} (i.e. 2.5, 5 and 10 mM Ca^{2+}, respectively). In 200 mg/L Ca^{2+}, the highest adsorbed amount (Γ) of EPS (1.1 mg/m^2) was obtained and the adsorption was irreversible. This Ca^{2+} concentration was also obtained by Zhu et al. [46] as the optimum concentration for EPS deposition on silica using quartz crystal microbalance with dissipation (QCM-D), in lieu of an optical reflectometer.

Lower adsorbed amounts (Γ = 0.6 mg/m^2 each) were obtained in the 100 and 400 mg/L Ca^{2+} solutions. This suggests that in both solutions, there was insufficient Ca^{2+} available for binding between the EPS and the silica surface. In the 100 mg/L Ca^{2+} solution, the adsorption reached an equilibrium faster than the other two solutions (Fig. 6). However, the maximum adsorbed amount of 1.1 mg/m^2 was not attained, perhaps due to insufficient Ca^{2+} to form complete polymer-surface bridges. On the other hand, above the optimum Ca^{2+} concentration required for adsorption (in the case of 400 mg/L Ca^{2+}), Lee et al. [47] described the occurrence of polymer–polymer binding instead of polymer-surface binding, which hampers the irreversible anchoring of polymers to surfaces (illustrated in Fig. 7). This phenomenon was substantiated by the desorption that occurred after the solvent injection in Fig. 6 (the vertical grey line).

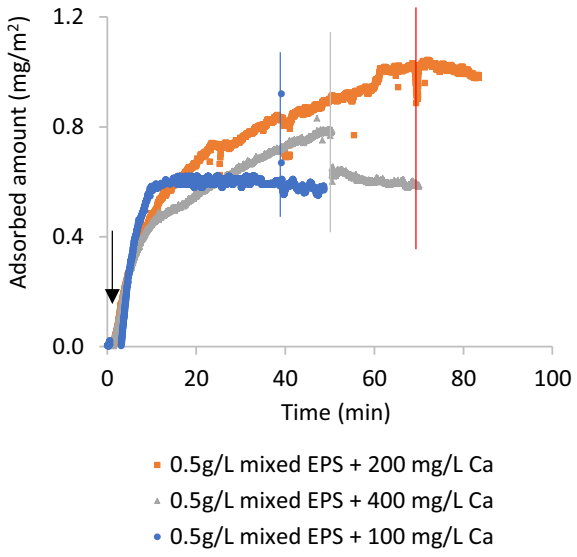

Fig. 6. Adsorbed amounts of mixed EPS dissolved in solutions of different Ca^{2+} concentrations on a silica surface. The black arrow is the point of EPS injection after establishing the baseline with the solvent (Ca^{2+} solution); the coloured vertical lines are the points of solvent injection after EPS adsorption on the surface: blue line for 100 mg/L Ca^{2+}, grey line for 400 mg/L Ca^{2+} and red line for 200 mg/L Ca^{2+}.

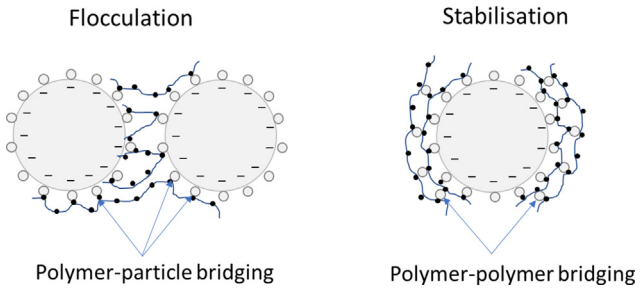

Fig. 7. Lee et al.'s [47] illustration of anionic polymer adsorption on kaolinite for two different types of divalent cationic bridging (flocculation and stabilisation).

It is worth mentioning that the optimum Ca^{2+} concentration and EPS surface coverage areas for the reflectometry and flocculation tests are different because, while the former involves an 'overdose' polymer regime, the latter operates in an 'underdose' or 'starved' polymer system. In reflectometry, the maximum adsorbed amount (a fully covered surface) is measured while in the flocculation process, a low surface coverage (low adsorption density) is needed [14] because a polymer adsorbed on one particle should be able to find a free spot on another particle. Comparing the optimum concentration of mixed EPS adsorbed on the clay particles (0.012 mg/g kaolinite and 0.018 mg/g montmorillonite – Section 3.3) with the maximum adsorbed amount (Γ) on the silica surface (0.6 mg/m^2 at 0.5 g/L EPS and 100 mg/L Ca^{2+}), the optimal mixed EPS surface coverage for good flocculation was about 2% for kaolinite and 3% for montmorillonite.

3.4.2. Adsorption of mixed EPS and its fractions

At the optimum Ca^{2+} concentration (200 mg/L Ca^{2+}), varying concentrations of mixed EPS (0.1–2.0 g/L) were adsorbed on the silica surface to establish an adsorption isotherm. Fig. S2 (see Supplementary material) shows that the isotherm reached a plateau at EPS concentrations above 0.5 g/L, with no significant difference in the adsorbed amounts at these concentrations (~1.1 mg/m^2). Hence, 0.5 g/L was used as the optimum EPS concentration (for the study of the maximum adsorbed amounts by reflectometry) for the mixed EPS, and also the HMW and MMW EPS since these three EPS types had the same optimum flocculation dosage (0.1 mg/g kaolinite and 0.5 mg/g montmorillonite).

Each EPS fraction had a lower irreversible adsorbed amount than the mixed EPS. The HMW, MMW and LMW EPS had irreversible Γ values of 0.79, 0.42 and 0.49 mg/m^2 at concentrations of 0.5, 0.5 and 1 g/L, respectively, (Table 4). Out of these three fractions, only the HMW EPS did not desorb significantly after rinsing with the solvent (Fig. S3). The MMW-EPS (at a concentration of 0.5 g/L) desorbed from 1.0 to 0.42 mg/m^2 (Fig. 8B) while the 0.5 g/L LMW EPS was completely desorbed (from 1.5 mg/m^2 before solvent injection to 0 mg/m^2 after solvent injection). However, the adsorbed amount of LMW EPS was concentration-dependent. At 1 g/L, about 2.8 mg/m^2 of LMW-EPS was adsorbed on the silica surface, out of which 0.49 mg/m^2 was irreversible (Fig. 8A). Hence, 82% of the initial adsorbed amount was desorbed as opposed to 58% for the MMW-EPS.

Table 4
Adsorbed amounts (Γ, n = 2) of mixed EPS and its fractions on silica surface in the presence of 200 mg/L Ca^{2+}. Unless otherwise stated (denoted as [a]), all Γ values were taken after solvent injection (irreversible adsorbed amounts). Hence, values with the superscript '[a]' are those before the solvent injection.

EPS (fraction)	EPS concentration (g/L)	Ca^{2+} concentration (mg/L)	Γ (mg/m^2)	Γ (μeq/m^2)
Mixed EPS	0.5	200	1.07 ± 0.02	5.43 ± 0.11
HMW EPS	0.5	200	0.79 ± 0.01	5.07 ± 0.08
MMW	0.5	200	1.00 ± 0.03 [a]	
MMW	0.5	200	0.42 ± 0.02	2.15 ± 0.05
LMW	0.5	200	1.50 ± 0.05 [a]	
LMW	0.5	200	0.00	
LMW	1.0	200	2.78 ± 0.15 [a]	
LMW	1.0	200	0.49 ± 0.01	0.64 ± 0. 02
LMW, then HMW	1.0, 0.5	5	0.49, 1.20	

[a] Adsorbed amount before solvent (200 mg/L Ca^{2+}) injection.

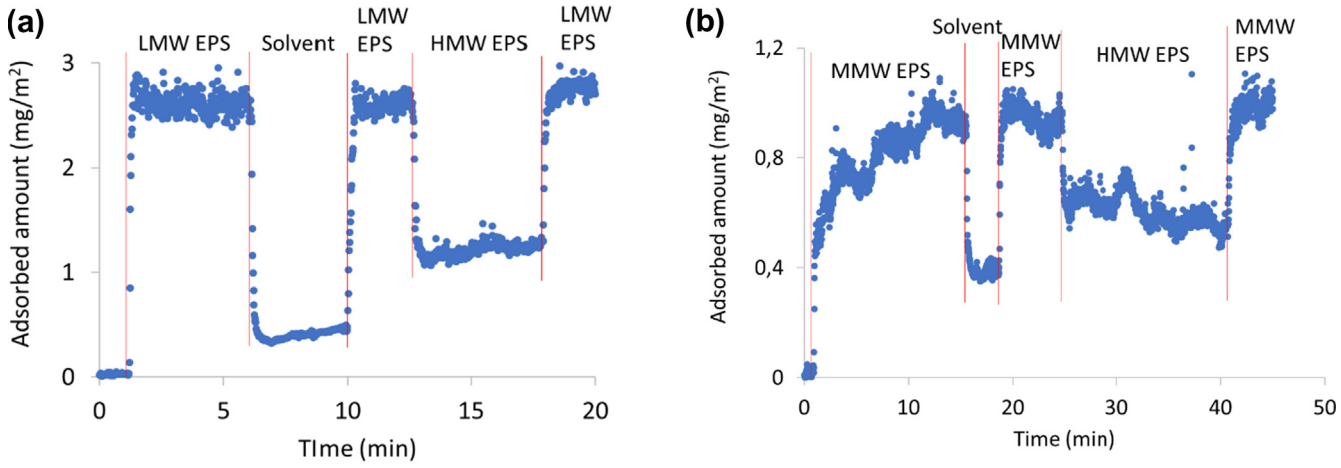

Fig. 8. A. Subsequent adsorption of HMW EPS fraction (0.5 g/L) fraction on pre-adsorbed LMW EPS (1.0 g/L) B. Subsequent adsorption of HMW EPS fraction (0.5 g/L) on pre-adsorbed MMW EPS fraction (0.5 g/L).

Each EPS fraction also displayed different adsorption rates, in the order LMW EPS > MMW EPS > HMW EPS (Table 5). The LMW EPS (composed of short polymeric chains relative to the other fractions) were rapidly deposited on the silica surface, with an initial adsorption rate, $[d\Gamma/dt]_0$ of 0.41 mg/m^2/s, followed by the MMW EPS with a $[d\Gamma/dt]_0$ of 0.096 mg/m^2/s. The $[d\Gamma/dt]_0$ of the HMW EPS and the mixed EPS were much lower (0.0004 mg/m^2/s for the HMW EPS and 0.0012 mg/m^2/s for the mixed EPS).

To obtain more information on the adsorption mechanism, we compared the initial adsorption rate, $[d\Gamma/dt]_0$ with the rate at which the polymers arrived at the interface (silicon wafer), given by the theoretical flux (J) [37]. When at the initial stage of the adsorption process, all the molecules that arrive the interface do adsorb, then $[d\Gamma/dt]_0 = J$. Table 5 shows that both the initial adsorption rate and the theoretical flux are inversely proportional to the MW (and most likely, the chain length) of the EPS fractions. About 85% of the LMW EPS molecules and 81% of the MMW EPS molecules that arrived at the interface adsorbed while only 0.4% of the HMW EPS molecules were adsorbed.

Table 5
The initial adsorption rate, $[d\Gamma/dt]_0$ and the rate at which each EPS fraction arrived at the interface (theoretical flux, J).

EPS (fraction)	Initial adsorption rate, $[d\Gamma/dt]_0$ (mg/m^2/s) (%)	Theoretical flux, J (mg/m^2/s)	Percentage of polymer adsorbed at the interface
LMW EPS	0.41	0.48	85
MMW EPS	0.096	0.12	81
HMW EPS	0.0004	0.10	0.4

It is worth mentioning that each of the EPS fractions (LMW, MMW and HMW) was somewhat polydisperse and the mixed EPS was very polydisperse. As J is directly proportional to the diffusion coefficient D [37], this means that small molecules (with a relatively high D) arrive at the surface first and thus, the adsorption kinetics is dominated by the smallest molecules within the EPS fraction. However, D was determined by dynamic light scattering (see supplementary material) and this technique is governed by the largest (and slowest) molecules because these scatter light the most. Hence, it is possible that we underestimated the flux of the molecules towards the surface and overestimated the percentage of polymers that adsorbed at the interface. However, we may safely conclude from the results in Table 5 (specifically from the percentage of EPS fractions adsorbed at the interface) that the adsorption kinetics of the LMW and MMW EPS fractions were (at least) mass transport-limited, while the adsorption kinetics of the HMW EPS fraction must have been limited by other factors aside mass transport, such as the unfolding of the polymer or conformational transitions [14].

4. Discussion

4.1. Mixed EPS characteristics

Since bacterial EPS, particularly wastewater-produced EPS, are a heterogeneous mixture of biomacromolecules, understanding the properties of each MW fraction is crucial in gaining insights into their flocculation behaviour. We can determine if it is expedient to extract the individual fractions (particularly the HMW fraction)

for single or mixed clay flocculation or to use the produced mixed EPS without further fractionation.

Having shown in previous studies that nitrogen limitation coupled with a relatively short solids retention time (1–3 days) is essential for increased EPS recovery from wastewater [28,48], the outcome of such a strategy, as also shown in this study, is the production of polysaccharide-rich mixed EPS with low protein content (at least when glycerol/ethanol-rich wastewater is used as the substrate). In addition, the results of this study reveal that about 93 wt % of the biopolymers are in the high and medium MW range, from which 84% are polysaccharides. These two fractions (the HMW and MMW EPS), majorly comprising polysaccharides, are largely responsible for the overall high MW (1.68 MDa) and charge density (5.10 meq/g) of the mixed EPS (Table 3) and determine its flocculation capacity. The MW of the produced mixed EPS tested in this study is within the range (500–2000 kDa) reported for other exopolysaccharides such as alginate and xanthan gum [49]. Extracellular proteins, on the other hand, are typically in the LMW range (10–250 kDa) [28,50] and have also been reported to play a critical role in flocculation [51]. Hence, the effect of protein-rich LMW EPS fraction on particle adsorption could not be overlooked and was studied alongside the polysaccharide-rich MMW and HMW EPS fractions.

4.2. Adsorption and flocculation of single clay particles

Preliminary flocculation tests done in the absence of Ca^{2+} showed, as expected, that EPS, having a net negative charge, could not flocculate negatively charged particles (such as kaolinite and montmorillonite) suspended in a medium of low ionic strength or one void of multivalent cations [7,33,46]. This is due to the electrostatic repulsion between the polymer adsorption sites and the clay particles according to the classical DLVO theory [7,46]. This phenomenon was confirmed with the zeta (ζ) potential measurements in Table S2 (supplementary material), which demonstrate that (i), the sole addition of EPS to the clay suspension did not increase the ζ potential value, as would be the case for cationic polymers [52]. This implies that the interaction between clay particles and EPS is governed by the presence of di/multivalent cations, whereby Ca^{2+}, for instance, can bridge between the anionic groups (COO^- – Table 2) of EPS and the negative sites of the clay particles [17]. (ii), above the optimum EPS dosage, the ζ potential values decreased due to the increasing concentration of non-adsorbed EPS in the supernatant (Fig. 4).

Above the optimum EPS dosage needed to flocculate the kaolinite particles, flocculation efficiencies decreased (Fig. 3A). This phenomenon has also been reported for the flocculation of kaolinite with excess anionic polyacrylamide [47]. During polyelectrolyte attachment to adsorption sites, bridges are developed between polymers and particles via divalent cationic bridging or hydrogen bonding [7,42]). Once the adsorption sites are occupied, higher polymer dosages result in higher concentrations of non-adsorbed polymer molecules in solution [47], as seen in Fig. 4. The effect of this is a reduction in particle flocculation because polymer–polymer bridges (which lead to stabilisation) become more dominant than polymer-particle bridges (which lead to flocculation), as illustrated in Fig. 7 [47]. Polymers with a relatively high CD (as found in the MMW, HMW and mixed EPS – Table 3) are more susceptible to this effect due to the presence of unoccupied sites that can engage in intramolecular bonding [7,28,47].

As regards montmorillonite flocculation with MMW, HMW and mixed EPS, colloid restabilisation did not occur at the tested dosages of 0.5–2.5 mg/g (Fig. 3B). A similar outcome has also been reported for montmorillonite and bentonite (the major fraction of bentonite is montmorillonite [53]) flocculation with anionic polyacrylamide [53], cationic polyacrylamide [33], non-ionic guar gum, non-ionic hydroxypropyl guar gum and cationic hydroxypropyl guar gum [54]. This implies that the absence of restabilisation in montmorillonite at increased polymer dosages is likely not governed by the polymer type, polymer charge or charge density but more related to the clay property. A possible explanation is the high cation exchange capacity of montmorillonite (Table 1), whereby Ca^{2+} (used as the coagulant in this study) can replace Na^+ in the clay, thereby increasing montmorillonite's adsorption sites for polymer-particle bridging, instead of polymer–polymer bridging that leads to stabilisation.

The LMW EPS (in the presence of 100 mg/L Ca^{2+}) might have been confined within the electrostatic repulsion layer because of their short polymeric chains [55], thus unable to effectively bridge between particles, leading to poor flocculation performances. The reflectometry tests further revealed that at low concentrations (<1 g/L), LMW EPS rapidly but reversibly adsorbed to the silica surface. In general, it is easier for small molecules to desorb from a surface due to their low binding affinity (as a result of their low adsorption energy per chain [37]), whereas, large polymers (with a high adsorption energy per chain) are bound to a surface by several 'trains' [17]. For desorption to occur, all trains of a chain must get loose at the same time, and the chance of this happening is smaller with increasing polymer length. At high concentrations of the LMW-EPS fraction ($\geq$1 g/L), the bigger polymers in this fraction are large enough to be irreversibly adsorbed (Table 4).

In the same vein, the MMW, HMW and mixed EPS induced particle flocculation. Apparently, the MW of these EPS types played significant roles in the flocculation process, especially when bridging is the underlying mechanism. This agrees with literature that flocculation is driven by 'high' MW components (>> 100 kDa) that can expand into the bulk and bridge with particles [17,40]. As observed in the adsorption tests, the mixed EPS and the HMW fraction were not desorbed after the solvent rinse. This irreversible adsorption is due to the strong attachment of the long polymeric and highly charged chains to the surface [37]. Although slow in the initial adsorption kinetics, the HMW polymers have a higher binding to the surface than the fast-adsorbing LMW and MMW fractions, and this may suggest that with time, the HMW EPS can replace the weakly bound smaller polymers. However, Fig. 8 A and B show that this is not the case.

Overall, the flocculation of single clay particles shows no significant differences among the performances of the MMW, HMW and mixed EPS types, although, for kaolinite, the HMW and mixed EPS would be preferred. More importantly, this study reveals that the presence of short polymeric chains (LMW EPS) in the harvested mixed EPS does not hinder its flocculation performance. Hence, mixed EPS can flocculate single clay particles as effectively as single-type HMW EPS.

4.3. Adsorption and flocculation in a dual particle system

One of the hypotheses prior to this study was that wastewater-produced mixed EPS (consisting of LMW, MMW and HMW fractions) can better flocculate a mixture of particles compared to the use of HMW EPS, perhaps due to the different MW fractions that may work synergistically for mixed particle flocculation.

The results in Fig. 5 show that mixtures of EPS can better flocculate mixed particles than the single HMW fraction. Furthermore, there is a 50% lower dosage requirement when using mixed EPS instead of the HMW EPS. The reflectometry results in Fig. 8A and B nicely explain the underlying adsorption mechanism of dual EPS fractions. Both figures reveal that the subsequent adsorption of the HMW EPS fraction did not displace the already adsorbed LMW and MMW EPS, which differs from what is found when homopolymers adsorb to silica surfaces [26]. For instance, the co-adsorption of the LMW and HMW EPS fractions in Fig. 8A resulted

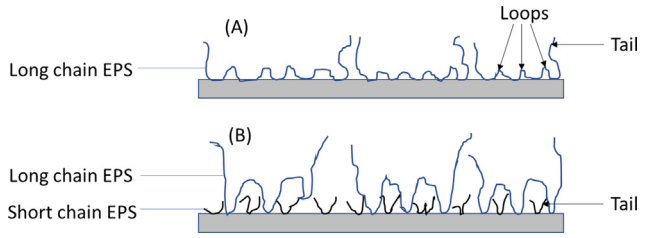

Fig. 9. (A) The expected configuration of an adsorbed HMW EPS fraction. (B) The co-adsorption of short (LMW EPS) and long (MMW or HMW) chain EPS fractions.

in a total adsorbed amount of 1.2 mg/m^2, a slightly higher value than the mixed EPS adsorbed amount (1.1 mg/m^2). The higher value may be due to the higher concentration of each tested EPS fraction compared to what was found in the harvested mixed EPS.

Additionally, the LC-OCD results in Table S3 (see supplementary material) also confirm the co-adsorption (rather than competitive adsorption) of both the LMW and HMW EPS fractions, and the MMW and HMW EPS fractions. At the optimum dosages, the EPS fractions were adsorbed in the flocs and their concentrations in the supernatant phase were found to be below the equipment's detection limit, even after concentrating the supernatant five times. However, above the optimum mixed EPS concentration (dosed concentration of 0.5 mg/g), not all the EPS fractions were adsorbed in the flocs. About 24.4 μg/L (=0.05 mg/g clay), attributed to the HMW EPS fraction, was measured in the supernatant phase.

Based on these results, we mechanistically deduce that when (mixtures of) particles are to be flocculated with mixed EPS comprising low, medium and high MW fractions, the LMW and MMW EPS, which are least affected by mass transport limitation, first adsorb to the (smallest) particles, while the HMW-EPS slowly attach to the bigger particles and the anchor sites of the LMW chains, both processes taking place in the presence of di/multivalent cations (Fig. 9). This mechanism is analogous to the 'site blocking' effect, which to the best of our knowledge, has only been reported for dual cationic polymer systems (typically composed of a LMW polymer that acts as a cationic site-blocking agent, and a cationic polymer) [14,56,57]. The vital component of this effect is the ability of the site-blocking agent (in our case, the LMW or MMW EPS fraction) to adsorb to the particle's surface site to which the flocculation polymer (the HMW EPS fraction) can adsorb (illustrated in Fig. 9) [56]. This effect is even more likely when both the site-blocking agent and the flocculation polymer have the same charge type, such that the former can adsorb to the same vacant sites that would have been available for the latter. The advantage of this effect is that the limited adsorption opportunity of the (HMW) flocculation polymer (as a result of site blocking) leads to more extended tails and enhanced bridging possibilities, thus improved flocculation.

A practical implication of these findings is that, it would not be necessary to further separate the HMW biopolymer fraction from the harvested EPS before they can be applied as effective flocculants. The harvested mixed EPS can effectively flocculate particles in single and dual clay systems, with performances comparable to the HMW EPS fraction during single clay flocculation, and a better performance than the HMW EPS during dual clay flocculation.

5. Conclusions

Wastewater-derived mixed extracellular polymeric substances (EPS), which are generally heterodispersed [7,13,15,16], were successfully fractionated into three molecular weight (MW) fractions [high (HMW), medium (MMW) and low (LMW) MW fractions] and each fraction was further characterised and examined to elucidate the flocculation mechanism of such complex biomacromolecules. This study shows that the MMW, HMW and harvested mixed EPS could effectively flocculate single clay systems, namely kaolinite or montmorillonite, in the presence of divalent cations. However, in a dual clay system, the mixed EPS proved to be more efficient (higher flocculation performance at a lower dosage) than the HMW EPS fraction, implying that the effect of mixed EPS on dual clay systems is higher than for single clay systems. The novel application of optical reflectometry on EPS, coupled with liquid chromatography-organic carbon detection (LC-OCD) analysis reveal site-blocking effect in EPS mixtures. Although this mechanism has been reported for dual cationic polymer systems [14,56,57], we show for the first time, the occurrence of the site-blocking effect for anionic mixed EPS in the presence of divalent cations. In this mechanism, the LMW and MMW EPS fractions, which were least affected by mass transport limitation, first adsorbed to the silica surface, while the HMW-EPS slowly attached to the unoccupied sites on the surface. We propose from this, a mixed EPS adsorption mechanism leading to extended anionic polymer tails in solution, thereby enhancing particle flocculation. Further research should be aimed at investigating the structure (including the degree of branching) of each EPS fraction and their influence on particle adsorption and flocculation. In addition, other factors influencing the flocculation process such as pH, ionic strength, ion composition and temperature should also be investigated.

CRediT authorship contribution statement

Victor Ajao: Conceptualization, Methodology, Validation, Investigation, Writing - original draft, Visualization. **Remco Fokkink:** Investigation, Resources, Writing - review & editing. **Frans Leermakers:** Writing - review & editing. **Harry Bruning:** Validation, Writing - review & editing, Supervision. **Huub Rijnaarts:** Validation, Resources, Writing - review & editing, Supervision, Project administration. **Hardy Temmink:** Conceptualization, Methodology, Resources, Writing - review & editing, Supervision, Project administration, Funding acquisition.

Declaration of Competing Interest

The authors declare that they have no known competing financial interests or personal relationships that could have appeared to influence the work reported in this paper.

Acknowledgments

This work was performed in the cooperation framework of Wetsus, European Centre of Excellence for Sustainable Water Technology (www.wetsus.nl). Wetsus is co-funded by the Dutch Ministry of Economic Affairs and Ministry of Infrastructure and Environment, the European Union Regional Development Fund, the Province of Fryslân and the Northern Netherlands Provinces. This work has also received funding from the European Union's Horizon 2020 research and innovation programme under the Marie Skłodowska-Curie [grant agreement No. 665874]. The authors thank the participants of the research theme 'Natural flocculants' for the fruitful discussions and financial support, and Claire Chassagne from Delft University of Technology for the zeta potential measurements.

Appendix A. Supplementary data

Supplementary data to this article can be found online at https://doi.org/10.1016/j.jcis.2020.07.146.

References

[1] C.S. Lee, J. Robinson, M.F. Chong, A review on application of flocculants in wastewater treatment, Process Saf. Environ. Prot. 92 (2014) 489–508, https://doi.org/10.1016/j.psep.2014.04.010.

[2] M. Lapointe, B. Barbeau, Dual starch–polyacrylamide polymer system for improved flocculation, Water Res. 124 (2017) 202–209, https://doi.org/10.1016/j.watres.2017.07.044.

[3] A. Mishra, M. Bajpai, Flocculation behaviour of model textile wastewater treated with a food grade polysaccharide, J. Hazard. Mater. 118 (2005) 213–217, https://doi.org/10.1016/j.jhazmat.2004.11.003.

[4] T. Suopajärvi, H. Liimatainen, O. Hormi, J. Niinimäki, Coagulation-flocculation treatment of municipal wastewater based on anionized nanocelluloses, Chem. Eng. J. 231 (2013) 59–67, https://doi.org/10.1016/j.cej.2013.07.010.

[5] F. Renault, B. Sancey, J. Charles, N. Morin-Crini, P.M. Badot, P. Winterton, G. Crini, Chitosan flocculation of cardboard-mill secondary biological wastewater, Chem. Eng. J. 155 (2009) 775–783, https://doi.org/10.1016/j.cej.2009.09.023.

[6] C. Wu, Y. Wang, B. Gao, Y. Zhao, Q. Yue, Coagulation performance and floc characteristics of aluminum sulfate using sodium alginate as coagulant aid for synthetic dying wastewater treatment, Sep. Purif. Technol. 95 (2012) 180–187, https://doi.org/10.1016/j.seppur.2012.05.009.

[7] V. Ajao, H. Bruning, H. Rijnaarts, H. Temmink, Natural flocculants from fresh and saline wastewater: Comparative properties and flocculation performances, Chem. Eng. J. 349 (2018) 622–632, https://doi.org/10.1016/j.cej.2018.05.123.

[8] H. Salehizadeh, N. Yan, Recent advances in extracellular biopolymer flocculants, Biotechnol. Adv. 32 (2014) 1506–1522, https://doi.org/10.1016/j.biotechadv.2014.10.004.

[9] T.T. More, J.S.S. Yadav, S. Yan, R.D. Tyagi, R.Y. Surampalli, Extracellular polymeric substances of bacteria and their potential environmental applications, J. Environ. Manage. 144 (2014) 1–25, https://doi.org/10.1016/j.jenvman.2014.05.010.

[10] S.A. Zaki, M.F. Elkady, S. Farag, D. Abd-El-Haleem, Characterization and flocculation properties of a carbohydrate bioflocculant from a newly isolated Bacillus velezensis 40B, J. Environ. Biol. 34 (2013) 51–58.

[11] G. Sathiyanarayanan, G. Seghal Kiran, J. Selvin, Synthesis of silver nanoparticles by polysaccharide bioflocculant produced from marine Bacillus subtilis MSBN17, Colloids Surfaces B Biointerfaces. 102 (2013) 13–20, https://doi.org/10.1016/j.colsurfb.2012.07.032.

[12] C. Liu, K. Wang, J.H. Jiang, W.J. Liu, J.Y. Wang, A novel bioflocculant produced by a salt-tolerant, alkaliphilic and biofilm-forming strain Bacillus agaradhaerens C9 and its application in harvesting Chlorella minutissima UTEX2341, Biochem. Eng. J. 93 (2015) 166–172, https://doi.org/10.1016/j.bej.2014.10.006.

[13] B. Bin Wang, X.T. Liu, J.M. Chen, D.C. Peng, F. He, Composition and functional group characterization of extracellular polymeric substances (EPS) in activated sludge: The impacts of polymerization degree of proteinaceous substrates, Water Res. 129 (2018) 133–142, https://doi.org/10.1016/j.watres.2017.11.008.

[14] J. Gregory, S. Barany, Adsorption and flocculation by polymers and polymer mixtures, Adv. Colloid Interface Sci. 169 (2011) 1–12, https://doi.org/10.1016/j.cis.2011.06.004.

[15] T.J. Stewart, J. Traber, A. Kroll, R. Behra, L. Sigg, Characterization of extracellular polymeric substances (EPS) from periphyton using liquid chromatography-organic carbon detection-organic nitrogen detection (LC-OCD-OND), Environ. Sci. Pollut. Res. 20 (2013) 3214–3223, https://doi.org/10.1007/s11356-012-1228-y.

[16] M. Ras, D. Lefebvre, N. Derlon, E. Paul, E. Girbal-Neuhauser, Extracellular polymeric substances diversity of biofilms grown under contrasted environmental conditions, Water Res. 45 (2011) 1529–1538, https://doi.org/10.1016/j.watres.2010.11.021.

[17] B. Bolto, J. Gregory, Organic polyelectrolytes in water treatment, Water Res. 41 (2007) 2301–2324, https://doi.org/10.1016/j.watres.2007.03.012.

[18] H.H.M. Rijnaarts, W. Norde, J. Lyklema, A.J.B. Zehnder, DLVO and steric contributions to bacterial deposition in media of different ionic strengths, Colloids Surfaces B Biointerfaces. 14 (1999) 179–195, https://doi.org/10.1016/S0927-7765(99)00035-1.

[19] A. Costine, J. Cox, S. Travaglini, A. Lubansky, P. Fawell, H. Misslitz, Variations in the molecular weight response of anionic polyacrylamides under different flocculation conditions, Chem. Eng. Sci. 176 (2018) 127–138, https://doi.org/10.1016/j.ces.2017.10.031.

[20] X. Yu, P. Somasundaran, Role of polymer conformation in interparticle-bridging dominated flocculation, J. Colloid Interface Sci. 177 (1996) 283–287 (accessed July 13, 2018) https://ac-els-cdn-com.ezproxy.library.wur.nl/S0021979796900338/1-s2.0-S0021979796900338-main.pdf?_tid=84eb5183-dd72-4d73-8131-748ea4d7be38&acdnat=1531487074_f06cf65017dbf974b71e48ad6aa99b64.

[21] Y. Sang, H. Xiao, Clay flocculation improved by cationic poly(vinyl alcohol)/anionic polymer dual-component system, J. Colloid Interface Sci. 326 (2008) 420–425, https://doi.org/10.1016/j.jcis.2008.06.058.

[22] S. Bárány, R. Meszaros, L. Marcinova, J. Skvarla, Effect of polyelectrolyte mixtures on the electrokinetic potential and kinetics of flocculation of clay mineral particles, Colloids Surfaces A Physicochem. Eng. Asp. 383 (2011) 48–55, https://doi.org/10.1016/j.colsurfa.2011.01.051.

[23] A. Fan, N.J. Turro, P. Somasundaran, A study of dual polymer flocculation, Colloids Surfaces A Physicochem. Eng. Asp. 162 (2000) 141–148, https://doi.org/10.1016/S0927-7757(99)00252-6.

[24] D.C. Sobeck, M.J. Higgins, Examination of three theories for mechanisms of cation-induced bioflocculation, Water Res. 36 (2002) 527–538, https://doi.org/10.1016/S0043-1354(01)00254-8.

[25] J.C. Dijt, M.A.C. Stuart, G.J. Fleer, Reflectometry as a tool for adsorption studies, Adv. Colloid Interface Sci. 50 (1994) 79–101, https://doi.org/10.1016/0001-8686(94)80026-X.

[26] J.C. Dijt, M.A.C. Stuart, G.J. Fleer, Competitive adsorption kinetics of polymers differing in length only, Macromolecules 27 (1994) 3219–3228, https://doi.org/10.1021/ma00090a015.

[27] L. Wågberg, I. Nygren, The use of stagnation point adsorption reflectometry to study molecular interactions relevant to papermaking chemistry, Colloids Surfaces A Physicochem. Eng. Asp. 159 (1999) 3–15, https://doi.org/10.1016/S0927-7757(99)00158-2.

[28] V. Ajao, S. Millah, M.C. Gagliano, H. Bruning, H. Rijnaarts, H. Temmink, Valorization of glycerol/ethanol-rich wastewater to bioflocculants: recovery, properties, and performance, J. Hazard. Mater. 375 (2019) 273–280, https://doi.org/10.1016/j.jhazmat.2019.05.009.

[29] W.F. Tan, W. Norde, L.K. Koopal, Humic substance charge determination by titration with a flexible cationic polyelectrolyte, Geochim. Cosmochim. Acta. 75 (2011) 5749–5761, https://doi.org/10.1016/j.gca.2011.07.015.

[30] V. Ajao, K. Nam, P. Chatzopoulos, E. Spruijt, H. Bruning, H. Rijnaarts, H. Temmink, Regeneration and reuse of microbial extracellular polymers immobilised on a bed column for heavy metal recovery, Water Res. 171 (2020), https://doi.org/10.1016/j.watres.2020.115472 115472.

[31] M. DuBois, K.A. Gilles, J.K. Hamilton, P.A. Rebers, F. Smith, Colorimetric method for determination of sugars and related substances, Anal. Chem. 28 (1956) 350–356, https://doi.org/10.1021/ac60111a017.

[32] T. Robert, S.M. Mercer, T.J. Clark, B.E. Mariampillai, P. Champagne, M.F. Cunningham, P.G. Jessop, Nitrogen-containing polymers as potent ionogens for aqueous solutions of switchable ionic strength: application to separation of organic liquids and clay particles from water, Green Chem. 14 (2012) 3053, https://doi.org/10.1039/c2gc36074h.

[33] S.M.R. Shaikh, M.S. Nasser, I.A. Hussein, A. Benamor, Investigation of the effect of polyelectrolyte structure and type on the electrokinetics and flocculation behavior of bentonite dispersions, Chem. Eng. J. 311 (2017) 265–276, https://doi.org/10.1016/j.cej.2016.11.098.

[34] G. Lagaly, S. Ziesmer, Colloid chemistry of clay minerals: The coagulation of montmorillonite dispersions, Adv. Colloid Interface Sci. 100–102 (2003) 105–128, https://doi.org/10.1016/S0001-8686(02)00064-7.

[35] P. Suresh Kumar, T. Prot, L. Korving, K.J. Keesman, I. Dugulan, M.C.M. van Loosdrecht, G.J. Witkamp, Effect of pore size distribution on iron oxide coated granular activated carbons for phosphate adsorption – Importance of mesopores, Chem. Eng. J. 326 (2017) 231–239, https://doi.org/10.1016/j.cej.2017.05.147.

[36] F. Mietta, C. Chassagne, A.J. Manning, J.C. Winterwerp, Influence of shear rate, organic matter content, pH and salinity on mud flocculation, Ocean Dyn. 59 (2009) 751–763, https://doi.org/10.1007/s10236-009-0231-4.

[37] J.C. Dijt, M.A.C. Stuart, J.E. Hofman, G.J. Fleer, Kinetics of polymer adsorption in stagnation point flow, Colloids Surfaces 51 (1990) 141–158, https://doi.org/10.1016/0166-6622(90)80138-T.

[38] A.R. Badireddy, S. Chellam, P.L. Gassman, M.H. Engelhard, A.S. Lea, K.M. Rosso, Role of extracellular polymeric substances in bioflocculation of activated sludge microorganisms under glucose-controlled conditions, Water Res. 44 (2010) 4505–4516, https://doi.org/10.1016/j.watres.2010.06.024.

[39] A. Barth, Infrared spectroscopy of proteins, Biochim. Biophys. Acta - Bioenerg. 1767 (2007) 1073–1101, https://doi.org/10.1016/j.bbabio.2007.06.004.

[40] S.J. Yuan, M. Sun, G.P. Sheng, Y. Li, W.W. Li, R.S. Yao, H.Q. Yu, Identification of key constituents and structure of the extracellular polymeric substances excreted by Bacillus Megaterium TF10 for their flocculation capacity, Environ. Sci. Technol. 45 (2011) 1152–1157, https://doi.org/10.1021/es1030905.

[41] B. Durmaz, F.D. Sanin, Effect of carbon to nitrogen ratio on the physical and chemical properties of activated sludge, Environ. Technol. 24 (2003) 1331–1340, https://doi.org/10.1080/09593330309385677.

[42] M.S. Nasser, A.E. James, The effect of polyacrylamide charge density and molecular weight on the flocculation and sedimentation behaviour of kaolinite suspensions, Sep. Purif. Technol. 52 (2006) 241–252, https://doi.org/10.1016/j.seppur.2006.04.005.

[43] S. Sam, F. Kucukasik, O. Yenigun, B. Nicolaus, E.T. Oner, M.A. Yukselen, Flocculating performances of exopolysaccharides produced by a halophilic bacterial strain cultivated on agro-industrial waste, Bioresour. Technol. 102 (2011) 1788–1794, https://doi.org/10.1016/j.biortech.2010.09.020.

[44] S. Cosa, A.M. Ugbenyen, L.V. Mabinya, K. Rumbold, A.I. Okoh, Characterization and flocculation efficiency of a bioflocculant produced by a marine Halobacillus, Environ. Technol. 34 (2013) 2671–2679, https://doi.org/10.1080/09593330.2013.786104.

[45] W.W. Li, W.Z. Zhou, Y.Z. Zhang, J. Wang, X.B. Zhu, Flocculation behavior and mechanism of an exopolysaccharide from the deep-sea psychrophilic bacterium Pseudoalteromonas sp. SM9913, Bioresour. Technol. 99 (2008) 6893–6899, https://doi.org/10.1016/j.biortech.2008.01.050.

[46] P. Zhu, G. Long, J. Ni, M. Tong, Deposition kinetics of extracellular polymeric substances (EPS) on silica in monovalent and divalent salts, Environ. Sci. Technol. 43 (2009) 5699–5704, https://doi.org/10.1021/es9003312.

[47] B.J. Lee, M.A. Schlautman, E. Toorman, M. Fettweis, Competition between kaolinite flocculation and stabilization in divalent cation solutions dosed with anionic polyacrylamides, Water Res. 46 (2012) 5696–5706, https://doi.org/10.1016/j.watres.2012.07.056.

[48] L. Faust, H. Temmink, A. Zwijnenburg, A.J.B. Kemperman, H.H.M. Rijnaarts, High loaded MBRs for organic matter recovery from sewage: Effect of solids retention time on bioflocculation and on the role of extracellular polymers, Water Res. 56 (2014) 258–266, https://doi.org/10.1016/j.watres.2014.03.006.
[49] P. Lembre, C. Lorentz, P. Di, Exopolysaccharides of the biofilm matrix: A complex biophysical world, in, Complex World Polysaccharides (2012), https://doi.org/10.5772/51213.
[50] B. Bin Wang, Q. Chang, D.C. Peng, Y.P. Hou, H.J. Li, L.Y. Pei, A new classification paradigm of extracellular polymeric substances (EPS) in activated sludge: Separation and characterization of exopolymers between floc level and microcolony level, Water Res. 64 (2014) 53–60, https://doi.org/10.1016/j.watres.2014.07.003.
[51] M.J. Higgins, J.T. Novak, Characterization of exocellular protein and its role in bioflocculation, J. Environ. Eng. 123 (1997) 479–485, https://doi.org/10.1061/(ASCE)0733-9372(1997)123:5(479).
[52] E.A. López-Maldonado, M.T. Oropeza-Guzmán, A. Ochoa-Terán, Improving the efficiency of a coagulation-flocculation wastewater treatment of the semiconductor industry through zeta potential measurements, J. Chem. 2014 (2014) 6–9, https://doi.org/10.1155/2014/969720.
[53] D. Liu, M. Edraki, L. Berry, Investigating the settling behaviour of saline tailing suspensions using kaolinite, bentonite, and illite clay minerals, Powder Technol. 326 (2018) 228–236, https://doi.org/10.1016/j.powtec.2017.11.070.
[54] B. Zhang, H. Su, X. Gu, X. Huang, H. Wang, Effect of structure and charge of polysaccharide flocculants on their flocculation performance for bentonite suspensions, Colloids Surfaces A Physicochem. Eng. Asp. 436 (2013) 443–449, https://doi.org/10.1016/j.colsurfa.2013.07.017.
[55] B.J. Lee, M.A. Schlautman, Effects of polymer molecular weight on adsorption and flocculation in aqueous kaolinite suspensions dosed with nonionic polyacrylamides, Water (Switzerland). 7 (2015) 5896–5909, https://doi.org/10.3390/w7115896.
[56] B. Brotherson, Y. Deng, Site blocking effect on the conformation of adsorbed cationic polyacrylamide on a solid surface, J. Colloid Interface Sci. 326 (2008) 324–328, https://doi.org/10.1016/j.jcis.2008.06.035.
[57] S. Behl, B. Moudgil, Control of active sites in selective flocculation III. Mechanism of site blocking, J. Collloid Interface Sci. 161 (1993) 430–436.